

Are all short-hard gamma-ray bursts produced from mergers of compact stellar objects?

Francisco J. Virgili and Bing Zhang

*Department of Physics and Astronomy, University of Nevada Las Vegas, Las Vegas, NV
89154, USA*

virgilif@physics.unlv.edu

zhang@physics.unlv.edu

Paul O'Brien

Department of Physics and Astronomy, University of Leicester, Leicester, LE1 7RH, UK

and

Eleonora Troja

*NASA Postdoctoral Program Fellow, Goddard Space Flight Center, Greenbelt, MD 20771,
USA*

ABSTRACT

The origin and progenitors of short-hard gamma-ray bursts remain a puzzle and a highly debated topic. Recent Swift observations suggest that these GRBs may be related to catastrophic explosions in degenerate compact stars, denoted as “Type I” GRBs. The most popular models include the merger of two compact stellar objects (NS-NS or NS-BH). We utilize a Monte Carlo approach to determine whether a merger progenitor model can self-consistently account for all the observations of short-hard GRBs, including a sample with redshift measurements in the Swift era (z -known sample) and the CGRO/BATSE sample. We apply various merger time delay distributions invoked in compact star merger models to derive the redshift distributions of these Type I GRBs, and then constrain the unknown luminosity function of Type I GRBs using the observed luminosity-redshift ($L - z$) distributions of the z -known sample. The best luminosity function model, together with the adopted merger delay model, are then applied to confront the peak flux distribution ($\log N - \log P$ distribution) of the BATSE and Swift samples. We find that for all the merger models invoking a range of merger delay time scales (including those invoking a large fraction of

“prompt mergers”), it is difficult to reconcile the models with all the data. The data are instead statistically consistent with the following two possible scenarios. First, that short/hard GRBs are a superposition of compact-star-merger-origin (Type I) GRBs and a population of GRBs that track the star formation history, which are probably related to the deaths of massive stars (Type II GRBs). Second, the entire short/hard GRB population is consistent with a typical delay of 2 Gyr with respect to the star formation history with modest scatter. This may point towards a different Type I progenitor than the traditional compact star merger models.

Subject headings: gamma rays: bursts — gamma rays: observations — methods: statistical

1. Introduction

Short-hard gamma ray bursts (GRBs) have been an enigma since the identification of a bimodal distribution in the CRGO/BATSE data by Kouveliotou et al. (1993). This study showed that GRBs are distributed into two populations with short (shorter than 2s) bursts having a harder spectrum and long (longer than 2s) bursts a softer spectrum, leading to the short-hard/long-soft classification. This purely observational division has a fair amount of scatter and does not necessarily indicate the nature of the intrinsic progenitor of a burst. Progress in understanding the progenitors of both long and short GRBs was made following the discoveries of their respective afterglows and host galaxies. While long bursts have been more securely shown to be associated with the collapse of massive stars (Hjorth et al. 2003; Stanek et al. 2003; Campana et al. 2006; Pian et al. 2006), the identification of a progenitor type for short-hard bursts has not been as successful. The most popular model is a merger event between two compact stellar objects, be it two neutron stars (NS-NS) or a NS and a black hole (NS-BH) (Lattimer & Schramm 1976; Paczynski 1986; Eichler et al. 1989; Narayan et al. 1992). This is supported by observational evidence of a *lack* of a supernova component in a handful of short-hard GRBs to deep limits (Hjorth et al. 2005; Covino et al. 2006; Kann et al. 2008) as well as the very important discovery of a handful of short bursts identified in non-star forming galaxies, such as GRBs 050509B and 050724, or at the edge of star forming galaxies, such as GRB 050709 (Gehrels et al. 2005; Bloom et al. 2006; Fox et al. 2005; Villasenor et al. 2005; Hjorth et al. 2005; Barthelmy et al. 2005; Berger et al. 2005). Such observational evidence, however, is not ubiquitous for all short GRBs. In fact, most short-hard GRBs discovered later are found in star forming galaxies or have missing hosts (Berger 2009).

Prompted by the discovery of GRB 060614, a nearby long GRB without an associated supernova but with many properties consistent with a merger-type progenitor (Gehrels et al. 2006; Gal-Yam et al. 2006; Fynbo et al. 2006; Della Valle et al. 2006), Zhang et al. (2007) suggest that the long vs. short classification of GRBs does not necessarily match the physical origins of massive star core collapse and mergers of compact stellar objects, respectively, and one needs multiple observational criteria to make correct identifications. The need of applying multiple criteria to determine the physical origin of a GRB was also discussed by Donaghy et al. (2006). Zhang et al. (2007) suggest naming GRBs with massive star progenitor and compact stellar object progenitor origins as “Type II” and “Type I”, respectively, so as to be differentiated from the traditional “long” and “short” terminology. A more elaborate physical classification scheme was discussed by Bloom et al. (2008). The multiple criteria to define Type II/I populations were elaborated in Zhang et al. (2009). They showed that not only could some long GRBs (such as GRB 060614) be of a Type I origin, but also that a good fraction (not only the Gaussian tail of the long population) of short GRBs could be of a Type II origin. They argued that the two recently discovered high- z GRBs with intrinsic short durations, GRBs 080913 and 090423, are most likely Type II bursts, and further suggested that some high- z , high- L short-hard GRBs can be of Type II origin as well. The goal of this work is to investigate through statistical methods whether the data are consistent with the hypothesis that “all short/hard GRBs are Type I”, in particular, whether they are related to compact star mergers.

Many of the specifics of Type I bursts are loosely constrained. Two important properties, among others, are the form of the luminosity function and the distribution of the merger delay time scale τ , which is defined as the time elapsed between star formation and the GRB. For compact star merger models, this is the delay between the formation of the two main sequence stars (i.e. the epoch of star formation) and the coalescence between the two evolved compact stellar objects (NS-NS or NS-BH). Several studies have endeavored to add constraints to these distributions (Ando 2004; Guetta & Piran 2005? ; Nakar et al. 2006b; Guetta & Piran 2006). For the merger delay time scale, usually a long delay is invoked, in the form of either a roughly constant delay (anywhere from 1-6 Gyr) or a distribution that is proportional to a power γ of the delay time scale τ . Nakar, Gal-Yam & Fox (2006b) constrained the delay distribution of merger events to $\tau > 4$ Gyr or a distribution $\propto \tau^{-0.5}$ or shallower, while Guetta and Piran (2006) concluded that this distribution can be modeled by a logarithmic delay or one with a constant delay, generally on the order of a few Gyr. Later, some short GRBs with much higher redshifts were identified (Berger 2007; Graham et al. 2009), which posed a challenge to the models invoking a long merger delay time scale. A more physical approach is to model the delay time scale through population synthesis (e.g. Belczynski & Kalogera 2001; Belczynski et al. 2002; Ivanova et al. 2003;

Dewi & Pols 2003; Belczynski et al. 2006). These authors suggest that merger timescales should not only be concentrated to long “classical” timescales (Bhattacharya & van den Heuvel 1991) but also include a prompt merger channel. These arguments stem from the details of the binary evolution process. Belczynski and Kalogera (2001) as well as Ivanova et al. (2003) and Dewi and Pols (2003) proposed a scenario where ultra-compact orbits can be achieved by an extra mass transfer event in the evolution of the binary, further reducing the orbital size of the final system that produces the bursts. This can lead to explosions on the order of 10s of Myr. This scenario is broadly consistent with the fact that short GRBs are seen in both early type galaxies and star forming galaxies (Belczynski et al. 2006; Zheng & Ramirez-Ruiz 2007; Zhang et al. 2009). However, it is unclear whether the model can reproduce all the available data of short-hard GRBs.

The luminosity function of Type I GRBs is even more sparsely constrained. Nakar et al. (2006b) assumed a simple powerlaw luminosity function and found that an index -2 can fit the available data by the end of 2005. Guetta & Piran (2006) introduced a broken powerlaw, with the indices in low luminosity ~ -0.5 and in high luminosity ranging from -1 to -2. Both works also included the caveat that the observational sample is very small, and that the data allows for some flexibility when combining rates, luminosities, and delay distributions. Modifications can also be added by considerations of multiple populations of short-hard bursts, such as a dual-peak luminosity function to account for local SGR giant flare events (Tanvir et al. 2005; Chapman et al. 2009), or the contributions of Type I GRBs from globular clusters (Grindlay et al. 2006; Salvaterra et al. 2008), but these contaminations are either not significant (Nakar et al. 2006a) or without robust evidence for their existence.

Since the early attempts of constraining compact star merger progenitor models (Nakar et al. 2006b; Guetta & Piran 2006) shortly after the discovery of the short GRB afterglows, the sample of short-hard GRBs with redshift measurements has significantly expanded. Observations after 2005 suggest that nearby, early-type galaxies are not common short GRB hosts, and that a significant fraction of short GRBs are likely from the high redshift universe (Berger et al. 2007; Berger 2009). Zhang et al. (2009) argued that the Type I Gold Sample, a small group of GRBs that carry direct evidence in favor of a compact stellar object origin, are not representative of the BATSE short-hard GRBs. In particular, four out of the five GRBs in the sample have extended emission, and all five have a moderate hardness ratio. Even without accounting for the extended emission, the “short spike” of GRB 050724 has a duration longer than 2 seconds. This GRB is the strongest evidence for the compact star merger origin of short GRBs to date, since its afterglow is within a nearby early type galaxy (Barthelmy et al. 2005; Berger et al. 2005). After 5 years of observations, however,

this burst is still the only one with such a robust association¹. Zhang et al. (2009) suspect that some (maybe even most) short-hard GRBs are not related to compact star mergers (Type I), but are related to deaths of massive stars (Type II). Recently, short GRB 090426 was discovered at $z = 2.6$. Several groups drew the conclusion that this burst is likely of a Type II origin based on some independent arguments (Levesque et al. 2009; Antonelli et al. 2009; Xin et al. 2010; Lü et al. 2010). Another related study is by Nysewander et al. (2009) (see also Kann et al. 2007, Kann et al. 2008), who analyzed the optical afterglow properties of both long and short GRBs and found that the two populations have very similar optical-to-X-ray flux ratios, suggesting that the average circumburst density of the two populations is similar. All these facts call for a serious re-investigation of the hypothesis that all short GRBs are related compact star mergers.

The current sample of short-hard GRBs with redshift measurements (the z -known sample) is large enough to serve the purpose of constraining redshift distribution and luminosity function of the population. This sample, together with the BATSE and Swift all short-hard GRB samples, can be used to perform a self-consistent check of the hypothesis that “all short-hard GRBs have compact binary merger progenitors”. This is the goal of this paper. Assuming that all the z -known short/hard GRBs detected in the Swift era are Type I GRBs, we perform a series of Monte Carlo simulations to constrain the luminosity function of these putative Type I GRBs by adopting several time delay distribution models, and check whether the same model can reproduce the peak flux distribution ($\log N - \log P$) of the BATSE and Swift samples. In §2 we detail the model assumptions and some information on the simulations. In §3 we present the results of the constraints on various models with different combinations of merger time delay distribution and luminosity function. Our results are summarized in §4 with a short discussion.

2. Models and Theoretical Framework

An advantage of utilizing numerical methods to approach a problem is that it can be easily broken down into its constituent parts for easy processing. The number of any type of GRBs that occur within a comoving volume element, dV/dz , per unit observed time at redshift $z \sim z + dz$ and luminosity $L \sim L + dL$ is given by

$$\frac{dN}{dt dz dL} = \frac{R_{GRB}(z)}{1+z} \frac{dV(z)}{dz} \Phi(L), \quad (1)$$

¹GRB 050509B (Gehrels et al. 2005; Bloom et al. 2006) is believed to be associated with a cD elliptical galaxy in a nearby cluster. However, the argument was based on a chance coincidence argument with the XRT error box, since no optical afterglow was detected for this burst.

with the factor of $(1+z)$ accounting for the cosmological time dilation, $R_{GRB}(z)$ being the GRB volume event rate (in unit of $\text{Gpc}^{-3} \text{yr}^{-1}$) as a function of z , $\Phi(L)$ the luminosity function, and $dV(z)/dz$ the comoving volume element given by

$$\frac{dV(z)}{dz} = \frac{c}{H_0} \frac{4\pi D_L^2}{(1+z)^2 [\Omega_M(1+z)^3 + \Omega_\Lambda]^{1/2}}, \quad (2)$$

for a flat Λ cold dark matter (Λ CDM) universe. Throughout the work, Ω_m and Ω_Λ are set to 0.3 and 0.7, respectively. Both the expressions for the GRB volume event rate ($R_{GRB}(z)$) and the luminosity function ($\Phi(L)$) of Type I bursts are unknown, and are the major focus of this study.

First, there is no theoretical prediction on the form of the luminosity function of Type I GRBs, which should in principle depend on the distributions of the masses of each member in the merging binary, the impact parameter, the collimation angle, and the viewing angle. Taking other astrophysical objects (e.g. long or Type II GRBs) as examples, we assume two general forms for the luminosity function for Type I GRBs, i.e. a powerlaw (PL)

$$\Phi(L) = \Phi_0 \left(\frac{L}{L_b} \right)^{-\alpha}, \quad (3)$$

or a smoothed broken powerlaw (BPL)

$$\Phi(L) = \Phi_0 \left[\left(\frac{L}{L_b} \right)^{\alpha_1} + \left(\frac{L}{L_b} \right)^{\alpha_2} \right]^{-1}, \quad (4)$$

where α , α_1 , and α_2 are the power law indices, L_b the break luminosity, and Φ_0 a normalization constant.

Second, the z -distribution of Type I GRBs can be modeled theoretically. For Type II GRBs, it is usually assumed that the volume rate of GRBs follows the star forming history, since the delay between the formation and death of a massive star is on the order of a few million years, much shorter than the variations in the cosmic star forming history or cosmological timescales. For Type I bursts, however, there is a delay, τ , between star formation and the GRB. In particular, for compact star merger scenarios, τ stands for the delay between the creation of the binary system, which follows the star forming history, and the eventual coalescence after the long decay of the binary's orbit via gravitational radiation. So the redshift distribution of Type I GRBs can be determined by the star forming history distribution convolved by a distribution of the delay time scale τ . This latter distribution is not fully established theoretically, and we test the following four models that have been discussed in the literature:

- Constant delay with dispersion: A δ -function like delay with the center value 1-5 Gyr, and a normal dispersion of $\sigma = 0.3$ or 1.0. These toy models are useful to gain insight on how different delay time scales meet the constraints of various models, but they are not very likely related to the true delay distribution for compact star mergers.
- Logarithmic delay: Delays with a distribution $P(\log(\tau))d\log(\tau) \sim \text{const}$, which implies $P(\tau) \sim 1/\tau$. This empirical form was adopted by Piran (1992), Guetta and Piran (2006), and Nakar, Gal-Yam and Fox (2006).
- Delay distribution from standard population synthesis: Belczynski et al. (2008) have modeled the NS-NS and NS-BH merger delay time scales using their population synthesis code. We have used their data and fit it with a 5th order polynomial and used this empirical model in our simulations. This model includes fast merger channels and allows for many short (< 100 Myr) mergers (see Fig.1). By applying this model, it is assumed that the metallicity evolution effect does not play a significant role in defining the delay time distribution of NS-NS and NS-BH mergers. This is evident by comparing the calculated merger delay time distributions between solar metallicity (Belczynski et al. 2006) and $\sim 1\%$ solar metallicity (Belczynski et al. 2008).
- Twin model for population synthesis: Belczynski et al. (2007) discussed another population synthesis model. This model incorporates the effect of twin binary systems (systems with almost equal mass stars) and is characterized by an even larger fraction of prompt mergers, with $\sim 70\%$ of the systems merging within 100 Myr, as opposed to $\sim 40\%$ in the previous population synthesis model. This most extreme prompt merger model would set an upper limit on the rate of prompt compact star mergers associated with star formation. We extract the delay distribution data from Belczynski et al. (2007), and simulate a distribution of burst using Monte Carlo techniques (Fig.1).

As will be evident later, most of the above models can interpret the short GRB data. We are then forced to consider the possibility that some or even most short GRBs are not Type I events but are instead related to massive stars (Type II). We therefore consider the following two redshift distribution models as well.

- No delay (Type II): In this model, short GRBs are assumed to follow star forming history of the universe, and are therefore related to deaths of massive stars (Type II). We consider two variations on such a model. First, we leave the luminosity function of these short Type II GRBs as unknown, and constrain it with the $L - z$ data. Second, we assume that these short Type II GRBs share the same luminosity function as long Type II GRBs, and use the established luminosity function of long Type II GRBs (Liang et al. 2007; Virgili et al. 2009) to perform the $L - z$ and $\log N - \log P$ tests.

- Mixed Type I/II distribution: The observed short GRBs are a combination of a Type I population (with a delay distribution defined by the standard population synthesis model (Belczynski et al. 2008) or the twin model (Belczynski et al. 2007) and a Type II population that follows the star forming history. The fraction of bursts in each population is a free parameter and can be constrained from the data.

Once the value of the delay is assigned (in units of Myr) it needs to be added to the previously simulated redshift to determine the redshift of the GRB. The redshift for the creation of the binary system, $z_{creation}$ is assumed to follow the star forming history and is assigned from the SF2 model of Porciani and Madau (2001)

$$R_{GRB} = 23\rho_0 \frac{e^{3.4z}}{e^{3.4z} + 22.0}. \quad (5)$$

This redshift is then used to calculate the cosmological look-back time by the following equation

$$\int_0^{z_{creation}} t(z) dz = \int_0^{z_{creation}} \frac{1}{H_0} \frac{1}{(1+z)(\Omega_m(1+z)^3 + \Omega_\Lambda)^{0.5}}. \quad (6)$$

With the values of this integral discretized over the simulated range ($z=0-10$) in units of Myr, we then subtract the merger time delay and re-convert to a redshift value with the same table. Those bursts with a negative lookback time (i.e. those that have not occurred yet) are discarded. The new redshift serves as the redshift of the merger and the GRB, z_{GRB} . Figure 2 shows how the redshift distribution (including the co-moving volume element and cosmological time dilation terms) is affected by different models of the merger timescale distribution.

With this formalism as a backdrop, we have enough information to create a set of bursts, each one defined with a unique and random (L, z) pair, which can then be passed through a series of filters that mimic a detector and then compared to the observed distribution. These simulations are similar to those conducted in Virgili et al. (2009), and here we summarize the most significant points.

Fundamentally, Monte Carlo simulations rely on random numbers, and although it is possible to create true random numbers with a device that uses a stochastic process (e.g. thermal noise), pseudo-random numbers are much more convenient in terms of ease of use and possibility for exact repetition of simulations. In this code we utilize the SIMD-oriented Fast Mersenne Twister, created by Mutsuo Saito and Makoto Matsumoto (Saito & Matsumoto 2008) of Hiroshima University. It is specifically designed for use with scientific Monte Carlo simulations, producing long strings of random numbers with a period of anywhere from $2^{607} - 1$ to $2^{216091} - 1$.

In order to compare the simulated output with observations, it is necessary to be in the same band as the detector with which one is observing (i.e. the k -correction). In order to achieve this, we assume every burst has a Band Function spectrum (Band et al. 1993), with spectral indices $\alpha = -1.0$ and $\beta = -2.3$ below and above a characteristic energy E_0 . Although some BATSE and Swift bursts have been adequately fit with an exponential cut-off power law (Ghirlanda et al. 2004; Sakamoto et al. 2008), this is very likely because the flux above E_p is too low to constrain the high energy photon index of the Band function. Recent Fermi observations suggest that for bright enough bursts, the Band function can fit the spectrum for both long (e.g. 080916C, Abdo et al. 2009a) and short bursts (e.g. GRB 090510, Abdo et al. 2009b). In the case of GRB 080916C, the Band spectrum extends several orders of magnitude in energy and supports our choice of the intrinsic spectrum for the simulated bursts. The characteristic energy correlates with the peak of the $\nu F(\nu)$ spectrum by the relation $E_p = E_0(2 + \alpha)$, which we assign from the relation proposed by Liang et al (2004) ²

$$E_p/200\text{keV} = C^{-1}(L/10^{52}\text{erg s}^{-1})^{1/2} \quad (7)$$

where C is randomly distributed in $[0.1, 1]$. This energy can then be used for the k -correction from the simulated bolometric luminosity in the rest-frame $1 - 10^4$ keV band (based on a certain luminosity function) into an arbitrary detector bandpass spanning the energy range (e_1, e_2) . The k -correction parameter is defined by

$$k = \frac{\int_{1/(1+z)}^{10^4/(1+z)} EN(E)dE}{\int_{e_1}^{e_2} EN(E)dE}. \quad (8)$$

The last step is to incorporate the detector threshold condition. For Swift, similar to Virgili et al. (2009), we apply the fluence threshold (Sakamoto et al. 2007)

$$F_{th} \sim (5.3 \times 10^{-9} \text{ erg cm}^{-2} \text{ s}^{-1})T_{90}^{-0.5} \quad (9)$$

in the 15-150 keV band as an approximation to the Swift trigger. This is because any valid rate trigger requires a statistically significant excess both in the rate and in the fluence domain, the latter being particularly stringent for short duration bursts. To calculate fluence from luminosity, we have randomly assigned a duration $T_{90}^{\text{short}} = 0.33 \pm 0.21\text{s}$ based on the BATSE sample statistics (Kouveliotou et al. 1993).

²Although this correlation was derived for long GRBs, it has been found that short GRBs share the similar $E_p - L$ correlation (Ghirlanda et al. 2009; Zhang et al. 2009). The $E_p - E_{\gamma,iso}$ correlations for the two categories are very different, mainly due to the shorter durations of short GRBs with respect to long GRBs.

Another test is the peak-flux distribution, i.e. $\log N - \log P$. Since redshift information is not needed, the sample is much larger. We consider both the Swift and BATSE short GRB samples. The latter is included because short GRBs were originally defined using the BATSE sample and if one wants to make the claim that “short GRBs are produced from compact star mergers”, one should make the case that both the BATSE and Swift short GRB samples are consistent with this hypothesis. For both distributions we filter the observational sample by utilizing a truncation in photon flux which is determined by the detector efficiency, as detailed in Loredo & Wasserman (1998), in order to provide an accurate statistical subsample of bursts. Both samples, coincidentally, have a cutoff of approximately $1 \text{ ph cm}^{-2} \text{ s}^{-1}$ above which the detector is sensitive, in the 50-300 keV and 1-1000 keV bands for BATSE and BAT, respectively (for BATSE see Loredo & Wasserman, for BAT see Band 2006, fig 3b). We apply this simple rate trigger to our simulated sample in order to compare similar subsamples. For the Swift sample, this is essentially consistent with the more complicated fluence trigger criterion discussed above for the $L - z$ constraints and we adopt this rate trigger criterion for the $\log N - \log P$ analysis for the sake of simplicity.

3. Results

The set of short bursts with known redshift is, to date, relatively small. We collect all the short GRBs with z information up to May 2009. The sample is compiled in Table 1. There are additional short bursts that have redshift claims (e.g. GRBs 000607, 051210, 060313, 060502B, 061201, 070809, and 080503), but we do not include them either because the redshift is uncertain, or because the burst is too faint to extract good spectral parameters so that no reliable luminosity can be derived. For the sample we present, we assume that the redshift values are all correct, but caution about the small chance of mis-identification due to afterglow/host chance coincidence (Cobb & Bailyn 2008). Among the highest redshift GRBs in this sample, GRB 070714B has $z = 0.923$ (Graham et al. 2009), and GRB 090426 has $z = 2.6$ (Levesque et al. 2009). GRB 060121 has two uncertain redshifts $z = 1.7, 4.6$ (de Ugarte Postigo et al. 2006), and we take the smaller value $z = 1.7$. Some studies (e.g. Berger et al. 2007; Berger 2009) suggest that there are more short bursts at these high redshifts. This would further strengthen the argument presented in this paper, namely, most short GRBs track the star formation history of the universe.

Utilizing the models presented in the previous section, we ran various sets of simulations combining different luminosity functions and time delay distributions. Varying the luminosity function parameters for a particular time delay distribution, one can compare the model predictions of GRBs in the $L - z$ space with the $L - z$ distributions of the data (see

Fig.3). Each comparison utilizes the 1D KS probability in z ($P_{KS,z}$), 1D KS probability in L ($P_{KS,L}$), and the total KS probability, defined as $P_{KS,t} = P_{KS,z} \times P_{KS,L}$. For a single power law LF (Eq.[3]), varying α leads to a distribution of $P_{KS,t}$ and the maximum $P_{KS,t}$ defines the most likely α value. Since the observed short GRBs seem to have an upper cutoff in the L distribution, it is more reasonable to adopt a smoothed broken power law LF (Eq.[4]). However, since there are three free parameters (α_1 , α_2 , and L_b), it is difficult to constrain all three parameters. We therefore fix $\alpha_2 = 2.5$, and constrain α_1 and L_b together using the $L-z$ criterion³. This results in a series of $P_{KS,t}$ contours in the (α_1, L_b) plane, an example of which is shown in Fig.4, from which we can infer the best fit parameters for that particular model. Using these parameters, we can then construct a simulated 2D $L-z$ graph with both the observed and simulated data plotted.

Our next constraint for the simulated bursts is consistency with the BATSE and Swift $\log N - \log P$ distributions. The BATSE 4B catalog (Paciesas et al. 1999) has 309 short bursts with $T_{90} < 2s$ (on a 64 ms timescale). When binned, the distribution gives a power law of slope of -1.12, extending from about 1-50 $\text{ph cm}^{-2} \text{s}^{-1}$ (in the 50-300 keV band), disregarding the turnover at low photon flux, which is likely an artifact of the detector. Adopting the 1 $\text{ph cm}^{-2} \text{s}^{-1}$ threshold as discussed above, we get a reduced BATSE short GRB sample with 271 bursts. This is the first sample we use to compare against simulation. The second sample is the Swift short GRB sample above the 1 $\text{ph cm}^{-2} \text{s}^{-1}$ count rate threshold. We get 31 bursts in this sample. The third sample includes all z -known Swift short GRBs above the 1 $\text{ph cm}^{-2} \text{s}^{-1}$ count rate threshold. This sample only has 12 GRBs.

For any z -distribution model, we adopt the most probable luminosity function derived by the $L-z$ constraint and simulate the $\log N - \log P$ distribution in the various detector bands. The simulated photon flux output is screened by a simple cut at the BATSE and Swift threshold of 1 $\text{ph cm}^{-2} \text{s}^{-1}$. The model results are compared with the observed data by the k -sample Anderson-Darling (AD) test (Scholz & Stephens 1987), which is more reliable than the KS or χ^2 tests when distributions have smaller numbers and/or might be drawing from the tails of the unknown underlying distribution. This test is similar to the KS test in that the null hypothesis is that the distributions come from the same underlying yet unknown distribution, but uses a more reliable test statistic. In order to accept the null hypothesis at the 95% confidence level, the statistic (which we call the T-statistic, see Table 2) must lie below a value of 1.96. In addition, the AD test is a test on the un-binned photon

³The reason of fixing α_2 is because the other luminosity function parameters (α_1 and L_b) have a greater effect on the simulated burst luminosity distributions (since the number of higher- L GRBs is much smaller than that of lower- L GRBs). We again follow the arguments in Liang et al. (2007) and Virgili et al. (2009) as guides in choosing a constant α_2 in the range of 2-2.5.

flux distribution, which is always more statistically reliable than the binned distribution. The figures are binned in log-log space for easy inspection and for consistency with the literature. The above procedure allows for a self-consistent check of every model through the joint $L - z$ and $\log N - \log P$ analysis. Any correct population model (including z distribution and luminosity function) should be able to show consistency in all data sets ($L - z$ distribution for the z -known short GRB sample, and the $\log N - \log P$ distribution of the BATSE and Swift short GRB samples).

Next we break down the results by merger time delay model and comment on the constraints imposed by the observations. Table 2 is a comprehensive list of test statistics and P-values for the relevant models in this analysis.

3.1. Constant merger time delay

We start with the constant merger delay models. The five models we considered are $\tau = 1, 2, 3, 4, 5$ Gyr, each with a gaussian scatter of 0.3 Gyr or 1.0 Gyr around these values. These models are not realistic compact star merger models. Most NS-NS systems in our galaxy have a predicted merger delay time scale longer than the Hubble time scale. Any realistic NS-NS merger delay time distribution model should include these systems. In any case, these models include a long time delay tail extending to Hubble time, and cannot be modeled by the constant delay models as discussed in this section. By studying these models, one would be able to diagnose how mergers at different delay time scales contribute to the global $L - z$ and $\log N - \log P$ distributions, so that the results invoking more complicated models (e.g. those invoking population synthesis) can be better understood.

Except for the 1-2 Gyr models, all other models demand a very shallow α_1 to account for the observed $L - z$ distribution. When combined with the corresponding z -distribution, this always leads to a very shallow BATSE $\log N - \log P$ that is inconsistent with the data. The reason is that the merger models give a clustering of bursts at low- z (Fig.2) so that the shape of the luminosity function carries significant weight in defining the shape of $\log N - \log P$. This is in contrast to the case of Type II GRBs, which are spread in a wide range of z so that the shape of luminosity function play a less important role in defining the shape of $\log N - \log P$ ⁴. The BATSE constraints show only the 2 Gyr model as passing the AD test. The constraints from the Swift sample, however, are much more forgiving for these models, allowing for 1-4 Gyr delays as acceptable fits. The results are insensitive to the assumed

⁴In an extreme, for a pure Euclidean geometry, the $\log N - \log P$ always has a slope of -3/2 regardless of the shape of luminosity function.

Gaussian scatter (0.3 Gyr vs. 1.0 Gyr). A breakdown of the various tests is illustrated in Fig. 7. By combining all the constraints, we conclude that only the 2 Gyr constant merger time delay model is consistent with the data.

3.2. Logarithmic and Population synthesis

More realistic compact star merger models are those that introduce a distribution of the merger delay time scales. We discuss the logarithmic distribution model and two more detailed models involving population synthesis (Belczynski et al. 2008; Belczynski et al. 2007). These models have the advantage to allow for a range of merger times that can lead to bursts in diverse host galaxy types.

The logarithmic and standard population synthesis models affect the redshift distribution in similar ways and have similar results in all tests, and are therefore discussed together. The constraints from the observed $L - z$ distributions all imply a very shallow luminosity function for these two models, generally having a slope of -0.2 or even larger, with moderate consistency (40-50%) for a broken power law luminosity function (see Fig.4). The reason for a shallow luminosity function is to avoid overproducing nearby low- L short GRBs. These shallow luminosity functions severely overproduce at high photon fluxes, giving a much shallower $\log N - \log P$ curve than observed. These models are therefore not favored by either the BATSE or Swift short GRB data.

The special population synthesis “twin model” as discussed above allows for an even larger fraction ($\sim 70\%$) of prompt mergers as compared to the standard population synthesis model ($\sim 40\%$). This affects the observed burst distribution by removing many of the higher merger timescale bursts and creating a distribution closer to one with no delay from the star forming history. This model has good consistency with the observed $L - z$ distributions and requires a steeper luminosity function slope than the previously discussed models. The $\log N - \log P$ is steeper as well, but not sufficiently steep for consistency with the BATSE sample, although consistency is achieved for the smaller Swift sample. Taking both constraints together, this model alone cannot adequately reproduce the observations.

3.3. No delay (Type II)

The above analysis leads us to conclude that the hypothesis that “all short GRBs detected by BATSE and Swift are of the compact star merger origin” is not justified, and that one needs to seriously explore alternative models. We first explore the other extreme,

namely, that all short GRBs track the star forming history of the universe. Similar to long GRBs, they are related to deaths of massive stars (Type II). Such a hypothesis is already disfavored by the host galaxy data of some short GRBs (e.g. Fong et al. 2010). We test this model mainly to see how close the real short GRB z -distribution is to the star formation history. We discuss two variations of this model. The first approach is to leave the luminosity function of these short Type II GRBs as unknown, and constrain it from the $L - z$ data. This approach is similar to the previous discussion of the other delay models. The implied slope of the luminosity function is, as expected from the general trend of steepening with decreasing delay time, steeper than the lowest constant τ model, weighing in at $\alpha_1 = 1.42$. The consistency with the observed $L - z$ distributions is low, about 20%, but not sufficient to completely rule out an association. The implied $\log N - \log P$ is inconsistent with observations for both the BATSE and the Swift samples (Fig 5a).

In the second approach, we also consider the possibility that these short Type II GRBs have a same parent population as the known long Type II GRBs, so that we can use the established luminosity function of long Type II GRBs (e.g. Liang et al. 2007; Virgili et al. 2009). As expected, this model is securely ruled out by the $L - z$ constraints although the $\log N - \log P$ distribution is consistent with the observations (see Fig. 5c).

In summary, attributing all short GRBs to Type II GRBs is not justified. This is expected since several Type I Gold Sample GRBs have been identified (Zhang et al. 2009), suggesting that at least some short GRBs should be of the Type I origin.

3.4. Mixed population model

Since the realistic compact star merger models detailed in the previous section are unable to reproduce all observational tests, we are forced to consider the possibility that the observed short GRBs include both compact star merger (Type I) events and events that are associated with massive stars (Type II). Although this possibility looks ad hoc at first sight, it may be already implied by the data. Zhang et al. (2009) discussed various criteria to assign a progenitor to a GRB and concluded that the often used T_{90} is not necessarily an informative parameter to define the physical category of a GRB. After discussing a series of multiple observational criteria, they applied the criteria that most directly carries the progenitor information and defined a Type I Gold Sample. They found that the Gold Sample bursts are relatively long (and most have extended emission), not particularly hard and that they are not a fair representation of the short hard GRB sample. On the other hand, none of the high luminosity short/hard GRBs have been found in elliptical or early type galaxies. Zhang et al. (2009) therefore speculated that some or even most high-luminosity short GRBs are

of the Type II origin. Our above analysis strengthens that conclusion and demands a more serious investigation of the mixed population in short GRBs.

We test this hypothesis by analyzing various merger timescale distributions that are a combination of Type I and Type II bursts. We consider a mix of Type I GRBs and the “classical” Type II GRBs, namely, those same Type II GRBs that account for the long-duration GRBs⁵. In this approach, the Type I bursts follow the distribution of merger delay time scales as predicted by the population synthesis models of Belczynski et al. (2008, 2007), and the Type II component tracks the star forming history of the universe and obey the known luminosity function of the long Type II population, as discussed in Virgili et al. (2009) and Liang et al. (2007). The logarithmic distribution is very similar to the standard population-synthesis derived distributions (Belczynski et al. 2008), so we do not discuss such an option explicitly.

We begin with the limiting case of 100% Type II GRBs. As mentioned in §3.3, this model (the “no delay” Type II model) shows good consistency with the observed $\log N - \log P$ distribution (Fig. 5c)⁶, but is securely ruled out by the $L - z$ constraints.

Next we test how different amounts of mixing can effect the distribution of bursts. To achieve this goal we do a series of simulations with different amount of mixing between the population synthesis Type I GRBs (based on the standard model of Belczynski et al. 2008) and the classical Type II bursts. A ‘20% mix’, for example, indicates 20% Type II and 80% Type I. The consistency with the $L - z$ constraints peaks around a 75% mix then falls off rapidly (with a few patches in the significance contours) near 90%. The corresponding $\log N - \log P$ distributions are plotted in Fig.5c together with the limiting case model composed entirely of classical Type II bursts. As shown, all models are too shallow or have hidden inconsistencies that are picked up with the AD test to be consistent with observations for the BATSE sample. This is expected in view of the lack of consistency with the un-mixed distribution. For the smaller Swift sample, the low mix models do equally as badly, but they begin to show consistency above 75%.

The “twin” population synthesis model (Belczynski et al. 2007) predicts an even higher fraction of prompt mergers ($\sim 70\%$ with $\tau < 100$ Myr), causing the redshift distribution to differ less from the one of pure Type II bursts. This is likely to affect the amount of mixing

⁵ In principle, the short Type II GRBs can be different from long Type II GRBs by having a different type of massive star progenitors. This would give too many unknown parameters to be constrained by the data.

⁶There is a small excess at the high photon flux end. In view of the log scale involved, this only gives an excess of bursts above $100 \text{ ph cm}^{-2} \text{ s}^{-1}$ that is below 2.

and the steepness of the $\log N - \log P$. We continue our analysis with the same procedure as the standard population synthesis model, slowly increasing the amount of mixing with the Type II bursts and observing how the results compare with the observations. As expected, the increase in prompt mergers decreased the amount of mixing needed for a good fit to the $L - z$ data. The peak probability is achieved for 20-30% Type II mixing, and a Type II mixing higher than 60% is securely ruled out by the $L - z$ data. The $\log N - \log P$ distribution is still too shallow up to a 30% mix to be consistent with the BATSE sample (Fig 5d). The Swift constraints are once again more forgiving, showing consistency with the 10-40% mix models. Taken together, we find consistency with the observed distributions in the 30-40% range for Type II mixing. Figure 8 shows a graphical breakdown of the tests for a 30% Type II mix model.

4. Conclusions and Discussion

With the extensive afterglow follow up observations of short GRBs in the Swift era, the sample of z -known GRBs has significantly expanded. This sample, together with the BATSE short GRB sample, can be used to constrain the luminosity function and redshift distribution of short GRBs by means of reproducing the observed $L - z$ distribution and $\log N - \log P$ distribution. In this paper, we have performed a detailed analysis on a list of models using Monte Carlo simulations. Our results can be summarized as follows:

- The hypothesis that “all short hard GRBs are of the compact star merger origin” is disfavored by the data. In particular, the merger time delay models derived from population synthesis (Belczynski et al. 2006, 2008, 2007) or using some empirical (e.g. logarithmic) formulae all demand a very shallow luminosity function in order to satisfy the $L - z$ constraint. This is because a steeper luminosity function would over-produce low- z , low- L short GRBs that are not observed. Such a required shallow luminosity function, combined with the redshift distribution derived from the merger delay time distribution, leads to a very shallow predicted $\log N - \log P$, which is inconsistent with the BATSE $\log N - \log P$ data.
- Among constant delay models, those with large delays (3-5 Gyr) suffer the same problem. Only the 2 Gyr model can satisfy both the $L - z$ and the $\log N - \log P$ (for both the BATSE and Swift samples, see Figs. 5 and 7) constraints. Such a model is however not a realistic model for compact star mergers, since most NS-NS binaries in our galaxies are found to have a merger delay time scale longer than Hubble time, not narrowly clustered near 2 Gyr.

- A model that invokes no merger delay (Type II) can better satisfy both the $L - z$ and $\log N - \log P$ constraints. However, a full consistency cannot be achieved. For a model invoking a Type II population with free luminosity function, the best fit luminosity function from the $L - z$ constraint predicts too steep a $\log N - \log P$ as compared with data. A model that invokes a luminosity function of the classical long Type II GRBs is securely ruled out, since it cannot reproduce the observed $L - z$ distribution.
- After considering the various tests detailed above, it seems that if one insists on the compact star merger model for (some) short GRBs, the data then demand a significant mixing of Type I and Type II GRBs in the observed short GRB population. This is in consistent with the argument presented in Zhang et al. (2009) who argued that the Type I Gold Sample is not a fair representation of the BATSE short/hard GRBs. For models mixing Type I bursts predicted from the standard population synthesis model and classical Type II bursts, no model can pass the BATSE $\log N - \log P$ test, and only models between 75% and 90% Type II mixing show consistency with the Swift $\log N - \log P$ and the $L - z$ constraints. For the most extreme “twin” population synthesis model invoking a much larger fraction of prompt mergers, consistency in all tests is achieved with a Type II mix of 30-40%. (See Figs. 5 and 8)

The above analysis indicates that there are two solutions for the short GRB z -distribution to satisfy the $L - z$ and $\log N - \log P$ constraints. The first one is ~ 2 Gyr constant delay distribution with some scatter. The second one is to have a wide range of delay time scales with respect to star formation, but the distribution is heavily tilted towards short delays, namely, over 80% short GRBs should have a delay time scale shorter than 100 Myr. This can be translated into two possible scenarios regarding the progenitor of short GRBs.

(1) If one takes the widely discussed compact star merger model for short GRBs, then this model alone cannot account for all short GRBs. This is because the compact star merger time scales cannot be clustered around 2 Gyr (in view of the galactic NS-NS population), and because any reasonable merger delay time scale distribution cannot give the high percentage ($> 80\%$) of prompt mergers. The standard population synthesis model only has $\sim 40\%$ such prompt mergers. The most extreme “twin” population synthesis model has a prompt merger fraction $\sim 70\%$, still not enough to satisfy the data constraints. Inevitably, one has to consider a superposition picture, namely, besides these merger-origin Type I GRBs, there are Type II GRB contamination in the short GRB population. Our analysis suggest that for the “twin” model, one still needs 30% – 40% Type II GRB contamination in the merger-origin Type I GRBs. The fraction of prompt mergers is therefore $(30\% + 70\% \times 70\%) - (40\% + 60\% \times 70\%) \simeq (79\% - 82\%)$ of events with delay time scale < 100 Myr. This is consistent with the general 80% constraint. We note Cui et al. (2010) obtained a similar

contamination fraction based on a different criterion (afterglow location in the host galaxy).

(2) Alternatively, the entire short GRB population may be related to a different type of progenitor with a typical delay time scale ~ 2 Gyr with respect to star formation history. Such a progenitor can be still of the Type I origin (explosions from compact stars), but is not from compact star mergers. One possible candidate may be accretion induced collapse of NS in binary systems (Qin et al. 1998; Dermer & Atoyan 2006).

Our analysis is based on L , z , and $\log N - \log P$ distributions of short GRB samples (both Swift and BATSE). There are other observational facts of short GRBs that are not considered in our modeling. Nonetheless, below we comment on how our results may be compatible with those observations.

- A small fraction of short GRBs have elliptical/early type host galaxies, the two best cases are GRB 050509B (Gehrels et al. 2005; Bloom et al. 2006) and GRB 050724 (Barthelmy et al. 2005; Berger et al. 2005). This is consistent with our suggestion that most short GRBs have short delay with respect to star formation.
- Fong et al. (2010) found that the relative location distribution of short GRBs in their host galaxies is different from that of long GRBs. Instead of tracking the brightest regions of the host galaxies, they under-represent the light distribution of their hosts. Their sample includes 10 GRBs, which are mostly nearby low-luminosity short GRBs. According to our first scenario (superposition scenario), the high-luminosity, high-redshift short GRBs are more likely Type II GRBs, but their host galaxies are not well studied. Even within the Fong et al. sample, most hosts are late-type galaxies. The difference with long GRBs in host location distribution only states that their progenitors are different from the long GRB progenitors. The short Type II GRBs can be related to other types of massive stars, which are different (e.g. in mass, spin, and/or metallicity) from the the progenitors of long Type II GRBs. Alternatively, according to our second scenario, all short GRBs may belong to a different type of Type I GRBs.
- Recent work by (Leibler & Berger 2010) suggest that delay times for short-hard bursts as derived from IR and optical observations of 19 bursts seem to imply different time delays for bursts occurring late- and early-type galaxies with median delays of ~ 0.2 and ~ 3 Gyr, respectively. The latter estimate, as well as an estimate for all galaxy types, falls within the limits of our 2 Gyr constant plus scatter models especially if one considers a large scatter around the median. It would be also consistent with our first scenario, namely, the observed population is a mix of a significant fraction of prompt

mergers along with some mix with Type II GRBs, along with a tail of long-delay mergers.

- Deep upper limits for SN association have been established in a few short GRBs. These are nearby low-luminosity short GRBs, which we also expect that they are of the Type I origin. So far there is no constraint on the SN association for high- L short GRBs. Some of these GRBs can be short Type II candidates according to our first scenario (superposition). According to our second scenario (2 Gy delay), all short GRBs are not expected to be accompanied by SNe.
- The metallicity of short GRB hosts is systematically different from that of long GRBs. Again the sample is mostly for nearby low-luminosity short GRBs. More data for high- z , high- L GRBs would help to distinguish between the two scenarios discussed in this paper.

Our results imply that if (some) short GRBs are from compact star mergers, the merger rate that give rise to short GRBs is smaller by 30% – 40% than previously estimated based on the assumption that all short GRBs are due to compact star mergers (e.g. Nakar et al. 2006b). If these merger events are also gravitational wave bursts, then the rate of gravitational wave bursts that are associated with GRBs is also lower by the same fraction. Alternatively, if short GRBs are not from compact star mergers, but from other Type I progenitors (e.g. accretion induced collapses). It is hopeful that the upcoming Advanced LIGO (Smith et al. 2009) experiment will be able to test these possibilities.

Our first scenario (superposition between Type I and Type II) also demands that within bursts of massive star origin (Type II), there could be two sub-types. One would need to find a reason to explain the apparent bimodal distribution in the T_{90} –hardness space. It may be related to the property of the progenitor star, or be related the process of launching a relativistic jet. The duration of a GRB is related to the duration of a relativistic jet that dissipates, which can be shorter than the total time scale of accretion (Zhang et al. 2009). Detailed models for short-duration Type II GRBs are called for (e.g. Lazzati et al. 2009).

As shown, important and robust conclusions can be drawn about the nature of short/hard bursts from the current observations. Increasing the sample of short/hard bursts, especially those with redshift measurements and clear host galaxy associations, is of the greatest importance toward understanding the diverse underlying progenitors of these bursts and how we come to observe them.

This work partially supported by NSF under grant AST-0908362, and by NASA under grants NNG05GB67G, NNX09AO94G, NNX08AE57A, NNX09AT66G, and through the

Nevada EPSCoR program (Nevada Space Grant). E.T. was supported by an appointment to the NASA Postdoctoral Program at the GSFC, administered by Oak Ridge Associated Universities through a contract with NASA. We would also like to thank Chris Belczynski for providing the redshift distribution data of NS-NS and NS-BH merger events from his population synthesis code, and Rob Preece, Josh Bloom, Rachid Ouyed, and Amei Amei for helpful discussion and comments.

REFERENCES

- Abdo, A. A. et al. 2009a, *Science*, 323, 1688
- Abdo, A. A. et al. 2009b, *Nature*, submitted
- Ando, S. 2004, *JCAP*, 06, 007
- Antonelli, L. A. et al. 2009, *A&A*, 507, L45
- Band, D., *ApJ*, 664, 378
- Band, D. L. et al. 1993, *ApJ*, 413, 281
- Barthelmy, S. D. et al. 2005, *Nature*, 438, 994
- Belczynski, K., Stanek, K. Z., Fryer C. L. 2007, arXiv:0712.3309
- Belczynski, K., Hartmann D. H., Fryer C. L., Holz, D. E., O’Shea, B. 2008, arXiv:0812.2470
- Belczynski, K., Kalogera V. 2001, *ApJ*, 571, 394
- Belczynski, K., Perna, R., Bulik T., Kalogera V., Ivanova, N., Lamb, D. 2006, *ApJ*, 648, 1110
- Belczynski, K., Bulik, T., Kalogera, V. 2002, *ApJ*, 571, 147
- Berger, E. 2009, *ApJ*, 690, 231
- Berger, E. 2007, *ApJ*, 670, 1254
- Berger, E. et al. 2007, *ApJ*, 664, 1000
- Berger, E. et al. 2005, *ApJ*, 634, 501
- Berger, E., et al. 2005b, *Nature*, 438, 988

- Bhattacharya, D., van den Heuvel, E. P. J. 1991, *Phys. Rep.*, 203, 1
- Bloom, J. S., Butler, N. R., Perley, D. A. 2008, *AIPC*, 1000, 11
- Bloom, J. S. et al. 2007, *ApJ*, 654, 878
- Bloom, J. S. et al. 2006, *ApJ*, 638, 354
- Campana, S. et al. 2006, *Nature*, 442, 1008
- Castro-Tirado, A. J., et al. 2005, *A&A*, 439, L15
- Cenko, S. B. et al. 2008, *arXiv:0802.0874*
- Chapman, R., Priddey, R. S., Tanvir N. R. 2009, *MNRAS*, 395, 1515
- Cobb, B. E., Bailyn, C. D. 2008, *ApJ*, 677, 1157
- Covino, S. et al. 2006, *A&A*, 447, 5
- Cucchiara, A. et al. 2007, *GCN Circular*, 6665
- Cucchiara, A., Fox, D. B., Berger, E., & Price, P. A. 2006, *GRB Coordinates Network*, 5470, 1.
- Cui, X.-H., Aoi, J., Nagataki, S. 2010, *arXiv:1004.2302*
- D’Avanzo, P., et al. 2009, *A&A*, 498, 711
- Della Valle, M. et al. 2006, *Nature*, 444, 1050
- de Ugarte Postigo, A. et al. 2006, *ApJ*, 648, L83
- Dermer, C. D., Atoyan, A. 2006, *ApJ*, 643, L13
- Dewi, J., Pols, O. 2003, *MNRAS*, 344, 629
- Donaghy et al. 2006, *arXiv:astro-ph/0605570*
- Eichler, D., Livio, M., Piran, T., & Schramm, D. N. 1989, *Nature*, 340, 126
- Fong, W., Berger, E., Fox, D. B. 2010, *ApJ*, 708, 9
- Fox, D. B. et al. 2005, *Nature*, 437, 845
- Fynbo, J. P. U. 2006, *Nature*, 444, 1047

- Gal-Yam, A., et al. 2006, *Nature*, 444, 1053
- Gal-Yam, A., Nakar, E., Ofek, E., et al. 2008, *ApJ*, 686
- Gehrels, N. et al. 2006, *Nature*, 444, 1044
- Gehrels, N. et al. 2005, *Nature*, 437, 851
- Grindlay, J., Portegies Zwart, S., McMillan, S. 2006 *Nature Physics*, 2, 116
- Ghirlanda, G. et al. 2004, *A&A*, 422, L55
- Ghirlanda, G., Nava, L., Ghisellini, G., Celotti, A., Firmani, C. 2009, *A&A*, 496, 585
- Graham, J. F. et al. 2009, *ApJ*, 698, 1620
- Guetta, D., Piran T. 2005, *A&A*, 435, 421
- Guetta, D., Piran T. 2006, *A&A*, 453, 823
- Hjorth, J. et al. 2005, *Nature*, 437, 859
- Hjorth, J. et al. 2003, *Nature*, 423, 847
- Hullinger, D., et al. 2006, *GRB Coordinates Network*, 5142, 1
- Ivanova, N., Belczynski, K., Kalogera V., Rasio, F., Taam, R. E. 2003, *ApJ*, 592, 475
- Kann, D. A. et al. 2008, arXiv:0804.1959
- Kann, D. A. et al. 2010, *ApJ*, 720, 1513
- Kouveliotou, C. et al. 1993, *ApJ*, 413, L101
- Kocevski, D., et al. 2010, *MNRAS*, 404, 963
- Lattimer, J. M., Schramm, D. N. 1976, *ApJ*, 210, 549
- Lazzati, D., Morsony, B. J., Begelman, M. C. 2009, *ApJ*, 717, 239
- Leibler, C. N., Berger, E. 2010, *ApJ*, submitted (arXiv:1009.1147)
- Levan, A. J., et al. 2006, *ApJ*, 648, L9
- Levesque, E. M., et al. 2010, *MNRAS*, 401, 963
- Levesque, E. M., et al. 2009, *GRB Coordinates Network*, 9264, 1

- Liang, E. W., Zhang, B., Virgili, F. J., Dai, Z. G., 2007, *ApJ*662, 1111
- Liang, E. W., Dai, Z. G., Wu, X. F. 2004, *ApJ*, 606, L29
- Loredo, T. J., Wasserman, I. M. 1998, *ApJ*, 502, 75
- Lü, H.-J., Liang, E.-W., Zhang, B.-B., Zhang, B. 2010, *ApJ*, submitted (arXiv:1001.0598)
- McBreen, S., et al. 2010, *A&A*, 516, 71
- Nakar, E., Gal-Yam, A., Piran, T., & Fox, D. B. 2006a, *ApJ*, 640, 849
- Nakar, E., Gal-Yam, A., Fox, D. B. 2006b, *ApJ*, 650, 281
- Narayan, R., Paczynski, B., & Piran, T. 1992, *ApJ*, 395, L83
- Nysewander, M., Fruchter, A. S., Pe'er, A. 2009, *ApJ*, 701, 824
- Paciesas, W. S. et al. 1999, *ApJS*, 122, 465
- Paczynski, B. 1986, *ApJ*, 308, L43
- Palmer, D. et al. 2006, *GRB Coordinates Network*, 5076, 1
- Pian, E. et al. 2006, *Nature*, 442, 1011
- Piran, T. 1992, *ApJ*, 389, L45
- Porciani, C., Madau, P. 2001, *ApJ*, 548, 522
- Prochaska, J. X. et al. 2006, *ApJ*, 642, 989
- Qin, B., Wu, X., Chu, M., Fang, L., Hu, J. 1998, *ApJ*, 494, L57
- Rau, A., McBreen, S., Kruehler, T., Greiner, J. 2009, *GRB Coordinates Network*, 9353, 1
- Sakamoto, T. et al. 2008, *ApJS*, 175, 179
- Sakamoto, T. et al. 2007, *ApJ*, 669, 1115
- Salvaterra, R. et al. 2008, *MNRAS*, 388, L6
- Saito, M., Matsumoto, M. 2008, "SIMD-oriented Fast Mersenne Twister: a 128-bit Pseudorandom Number Generator", Monte Carlo and Quasi-Monte Carlo Methods 2006, Springer, 607
- Scholz, F. W., Stephens, M. A. 1987, *J. Amer. Statistical Assoc.*, Vol. 82, No. 399, 918

- Smith, J. R., LIGO Scientific Collaboration, 2009, *Classical and Quantum Gravity*, 26, 114013
- Stanek, K. Z. et al. 2003, *ApJ*, 591, L17
- Soderberg, A. M., et al. 2006, *ApJ*, 650, 261
- Tanvir, N. R., Chapman, R., Levan, A. J., Priddey, R. S., 2005, *Nature*, 438, 991
- Troja, E. et al. 2008, *MNRAS*, 385, L10
- Villasenor, J. S. et al. 2005, *Nature* 437, 855
- Virgili, F. J., Liang, E.-W., Zhang, B. 2009, *MNRAS*, 392, 91
- Xin, L.-P. et al. 2010, *MNRAS*, in press (arXiv:1002.0889)
- Zhang, B. et al. 2007, *ApJ*, 655, L25
- Zhang, B. et al. 2009, *ApJ*, 703, 1696
- Zheng, Z., Ramirez-Ruiz, E. 2007, *ApJ*, 665, 1220

Table 1: The z -known short/hard GRB sample

GRB name	z redshift	$L_{\gamma,iso}^{peak}$ $10^{50} \text{ erg s}^{-1}$
050509B	0.2248	$0.07_{-0.05}^{+0.10}$
050709	0.1606	$5.4_{-0.69}^{+0.67}$
050724	0.2576	$0.99_{-0.10}^{+0.23}$
060614	0.1254	$1.39_{-0.07}^{+0.13}$
061006	0.4377	$24.60_{-0.77}^{+1.22}$
050813	0.72	4.13 ± 2.02
051221A	0.5464	25.8 ± 0.9
060121	1.7/4.6	$2445 \pm 162/33574 \pm 2226^a$
060502B	0.287	0.65 ± 0.09
060801	1.131	$47.6_{-1.6}^{+6.2}$
061210	0.4095	21.5 ± 1.4
061217	0.8270	10.8 ± 1.8
070429B	0.9023	24.6 ± 3.8
070714B	0.9225	57.3 ± 3.6
070724A	0.457	$1.58_{-0.14}^{+0.34}$
071227	0.3940	3.34 ± 0.49
090426	2.6	171_{-44}^{+24}
090510	0.9	376_{-172}^{+186}

Note. — uminositities derived by author unless otherwise specified. References for redshift measurements: **GRB050509B**:(Gehrels et al. 2005), (Bloom et al. 2006), (Castro-Tirado et al. 2005); **GRB050709**:(Fox et al. 2005),(Covino et al. 2006),(Prochaska et al. 2006); **GRB050724**: (Berger et al. 2005b), (Prochaska et al. 2006); **GRB060614**: (Della Valle et al. 2006); **GRB061006**: (Berger et al. 2007); **GRB050813**: (Prochaska et al. 2006); **GRB051221A**: (Soderberg et al. 2006); **GRB060121**: (?)=1.7: levan06, (Berger et al. 2007), $z=4.6$: (de Ugarte Postigo 2006) **GRB060502B**:(Bloom et al. 2007); **GRB060801**:(Cucchiara et al. 2006), (Berger et al. 2007); **GRB061210**:(Berger et al. 2007); **GRB061217**: (Berger et al. 2007); **GRB070429B**: (Cenko et al. 2008); **GRB070714B**: (Graham et al. 2009), (Cenko et al. 2008); **GRB070724A**: (Cucchiara et al. 2007), (Berger 2009), (Kocevski et al. 2010); **GRB071227**: (D’Avanzo et al. 2009),(Berger 2009); **GRB090426**: (Levesque et al. 2009), **GRB090510**:(Rau et al. 2009), (McBreen et al. 2010); ^a We chose $z=1.7$ for this analysis; ^b Derived from $\frac{E_{\gamma,iso}}{T_{90}}$. T_{90} : (Palmer et al. 2006), $E_{\gamma,iso}$: (Hullinger et al. 2006);

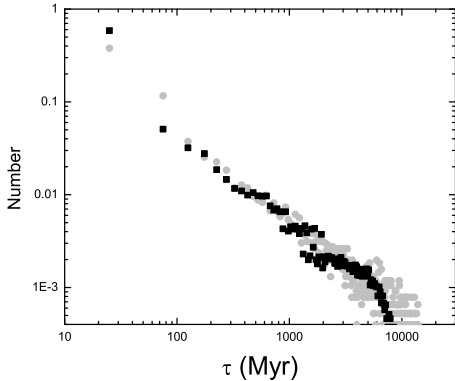


Fig. 1.— A comparison of the simulated merger delay time distributions between the standard population synthesis model (Belczynski et al. 2008, grey) and the “twin” population synthesis model (Belczynski et al. 2007, black). Note the higher fraction of prompt mergers in the twin model.

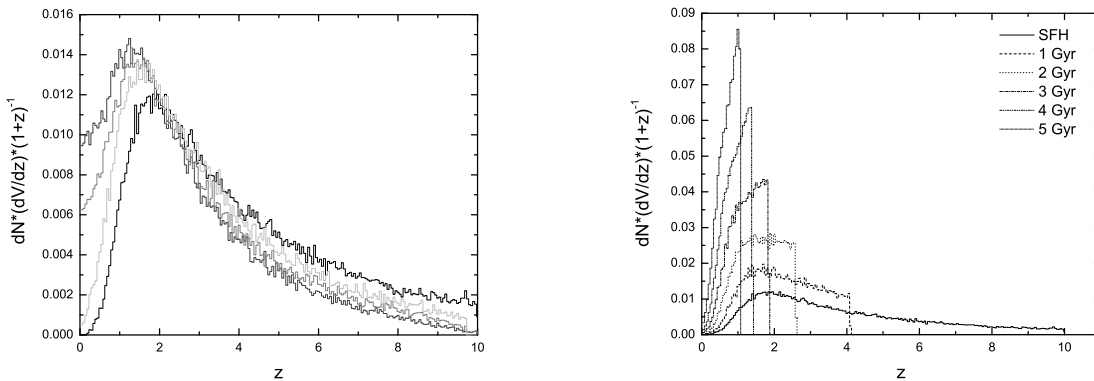


Fig. 2.— Modified GRB redshift distributions (Eq.[1] integrated over L) including the effects of cosmological time dilation and the comoving volume element, dV/dz . Different curves correspond to different models invoking different merger delay timescale distributions. The left panel shows a model that follows the star forming history (i.e. no merger time delay; black) as well as the population synthesis (standard, gray; twin, light gray) and logarithmic (dark gray) models. The right panel shows various constant delay models as compared with the no delay model. All histograms contain the same number of bursts.

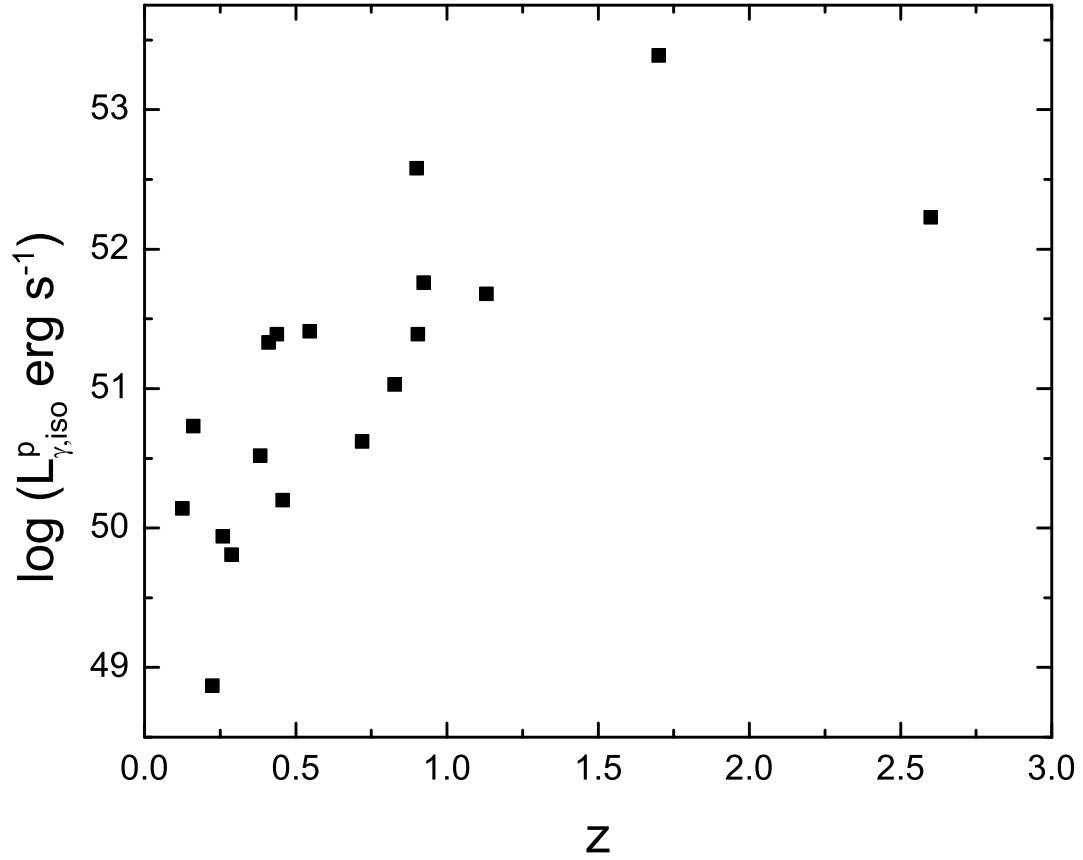


Fig. 3.— Sample of the z -known short-hard GRBs detected in the Swift era. The redshifts are plotted against peak isotropic gamma-ray energy, L . This distribution is used to constrain luminosity function of various redshift distribution models.

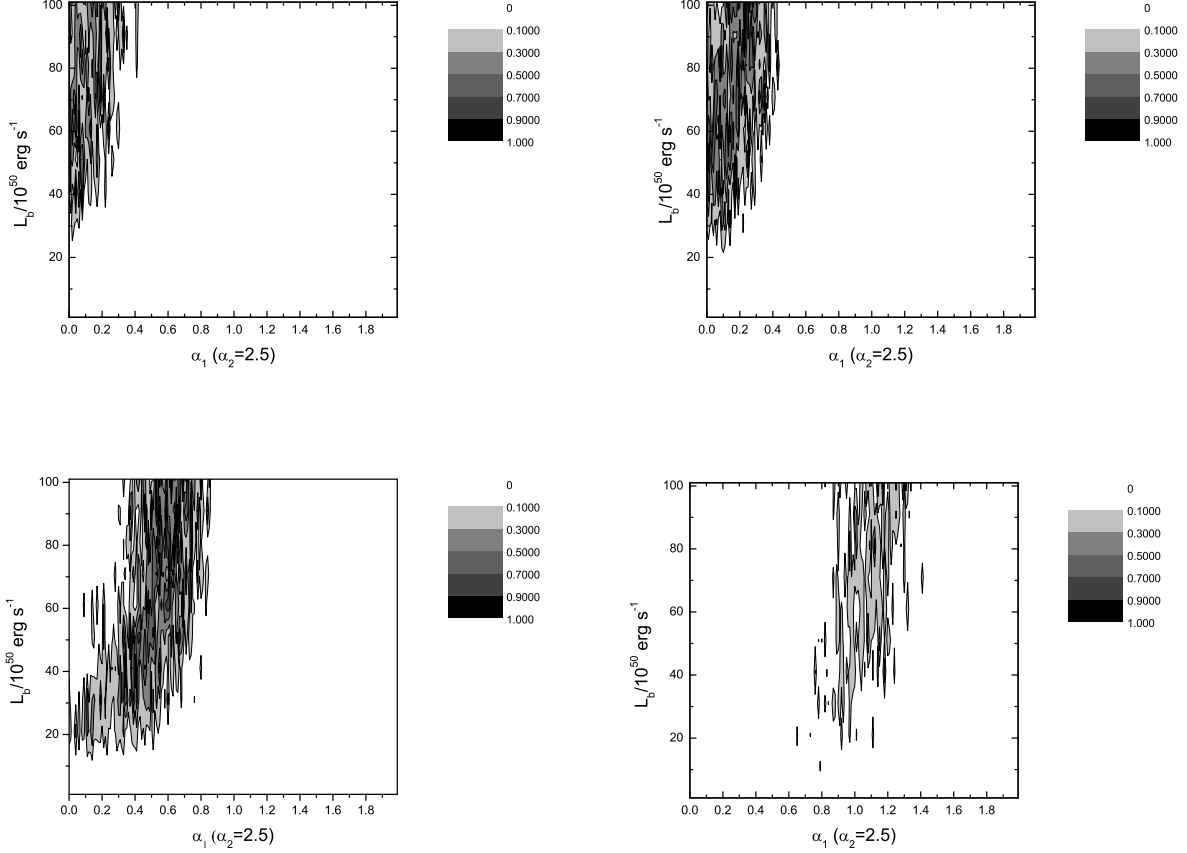


Fig. 4.— A series of contours displaying the total KS probability, $P_{KS,t}$ of varying luminosity function parameters (break luminosity, L_b and pre-break power-law slope α_1) derived from the $L - z$ constraints for a sample of redshift distribution models. (a) the logarithmic model, (b) the standard population synthesis model, (c) the “twin” population synthesis model, and (d) the no delay model. Darker indicates higher KS probabilities for consistency with the observed $L - z$ distribution.

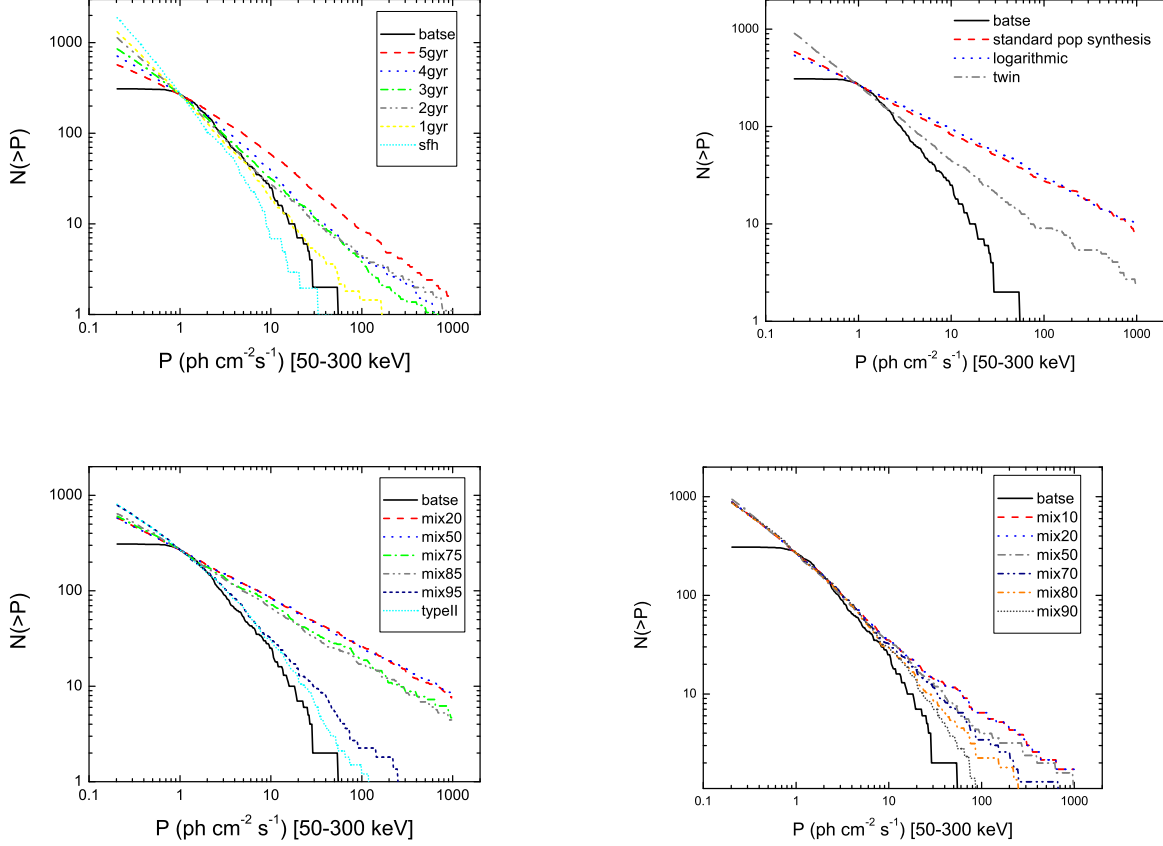


Fig. 5.— Comparison of the $\log N - \log P$ distributions for the various models with the observed BATSE curve. (a) various constant delay merger models ($\sigma = 0.3$ are shown. Curves for $\sigma = 1.0$ are similar and therefore not included in the figure); (b) the standard population synthesis, logarithmic and twin models. (c) mixed models with classical Type II’s (with long Type II luminosity function) and Type I’s with standard population synthesis time delay distribution; (d) mixed models with classical Type II’s and Type I’s with time delay distribution predicted by the “twin” population synthesis model. The notation “mix20” standards for 20% Type II (and 80% Type I) for both panels (c) and (d). Few models pass the BATSE constraints, with the exception of: (1) the 2 Gyr model (both $\sigma = 0.3$ and 1.0); and (2) the 30% and 40% Type II-twin mix models. See Table 2 for test statistics and P-values for various models.

Table 2: Summary of merger models and statistical tests

Model	LF parameters (α_1, L_B, α_2)	KS_z D-stat, Prob	KS_L D-stat, Prob	KS_t Prob	BATSE LNLP T stat, P-value	Swift LNLP ^a T stat, P-value
1 Gyr ($\sigma = 1.0$)	(0.7,60,2.5)	0.18, 0.69017	0.14, 0.91849	0.6339	2.12591, 0.04245	-0.50769, 0.47997
2 Gyr ($\sigma = 1.0$)	(0.42,40,2.5)	0.14222, 0.90913	0.18, 0.69017	0.6275	1.57805, 0.07254	-0.55567, 0.49462
3 Gyr ($\sigma = 1.0$)	(0.48,80,2.5)	0.11333, 0.98782	0.12667, 0.96301	0.9513	2.60683, 0.02702	0.41429, 0.22775
4 Gyr ($\sigma = 1.0$)	(0.19,40,2.5)	0.15333, 0.85484	0.15778, 0.8301	0.7096	7.75112, 0.00041	1.25399, 0.10017
5 Gyr ($\sigma = 1.0$)	(0.23,80,2.5)	0.17556, 0.71954	0.18, 0.69017	0.4966	22.48737, 0	6.75693, 0.00090
1 Gyr ($\sigma = 0.3$)	(0.93,80,2.5)	0.19556, 0.58666	0.17778, 0.7049	0.4135	4.70011, 0.00469	-0.36637, 0.4371
2 Gyr ($\sigma = 0.3$)	(0.68,90,2.5)	0.15333, 0.85484	0.16222, 0.80396	0.6873	1.44098, 0.08312	-0.69955, 0.53852
3 Gyr ($\sigma = 0.3$)	(0.42,30,2.5)	0.11556, 0.98491	0.15333, 0.85484	0.8419	2.67700, 0.02534	-0.61568, 0.51296
4 Gyr ($\sigma = 0.3$)	(0.35,50,2.5)	0.12889, 0.957	0.14444, 0.89924	0.8606	1.97297, 0.04921	0.25168, 0.26728
5 Gyr ($\sigma = 0.3$)	(0.35,50,2.5)	0.28, 0.17119	0.23333, 0.3608	0.0618	7.91458, 0.00036	5.38114, 0.00272
Population synthesis	(0.19,80,2.5)	0.14, 0.91849	0.12667, 0.96301	0.8845	45.97288, 0	3.72465, 0.01033
Logarithmic	(0.08,80,2.5)	0.15333, 0.85484	0.16444, 0.79044	0.6757	55.10492, 0	6.01050, 0.00164
No delay	(1.15,80,2.5)	0.19556, 0.58666	0.24667, 0.29602	0.17367	19.71989, 0	2.00273, 0.04781
Twin	(0.14,30,2.5)	0.20889, 0.50096	0.19111, 0.61609	0.30864	2.45747, 0.03102	-0.37388, 0.43936
Mix 20 (PS) ^b	(0.24,80,2.5)	0.16667, 0.77666	0.14, 0.91849	0.71336	32.62143, 0	3.77945, 0.00978
Mix 50 (PS)	(0.2,90,2.5)	0.15556, 0.84266	0.15111, 0.86662	0.7302	31.48321, 0	4.03421, 0.00798
Mix 75 (PS)	(0.07,30,2.5)	0.14444, 0.89924	0.12444, 0.96845	0.8709	29.94587, 0	3.41307, 0.01332
	(0.62,80,2.5)	0.19333, 0.60134	0.17556, 0.71954	0.4327	20.85024, 0	1.46488, 0.08117
Mix 85 (PS)	(0.2,30,2.5)	0.19556, 0.58666	0.11333, 0.98782	0.5795	17.84703, 0	1.30219, 0.09546
Mix 90 (PS)	(0.1,30,2.5)	0.273333, 0.192129	0.215556, 0.460233	0.0884	13.68442, 0	1.14002, 0.11223
Mix 10 (Twin)	(0.61,90,2.5)	0.11333, 0.98782	0.14, 0.91849	0.9073	1.70715, 0.06384	3.43719, 0.01305
Mix 20 (Twin)	(0.56,60,2.5)	0.10889, 0.99239	0.10889, 0.99239	0.9848	2.56935, 0.02796	-0.41484, 0.45173
Mix 30 (Twin)	(0.33,20,2.5)	0.16667, 0.77666	0.13556, 0.93559	0.7266	1.85675, 0.05511	-0.32577, 0.42493
Mix 40 (Twin)	(0.5,40,2.5)	0.24667, 0.29602	0.19111, 0.61609	0.1824	1.60761, 0.07044	-0.14547, 0.37216

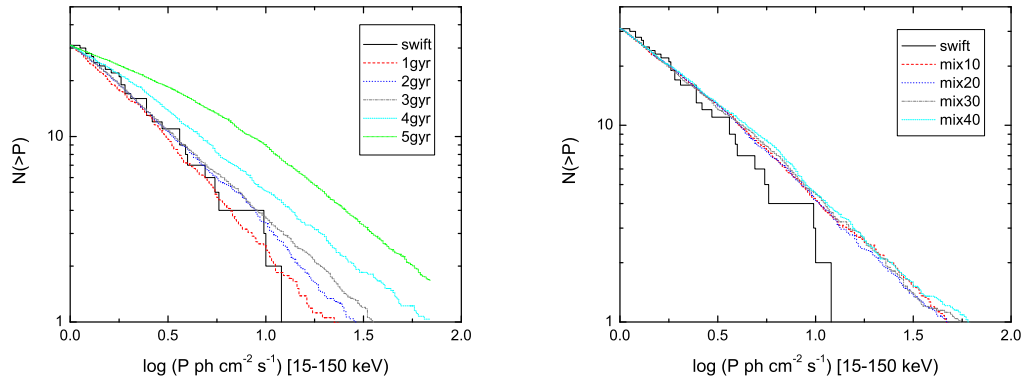


Fig. 6.— $\log N - \log P$ distributions for the observed Swift sample and the simulated bursts in the Swift (15-150 keV) band. Unlike the BATSE constraints, this test gives consistency for many more models and we present the most relevant ones here. The first panel shows constant merger models ($\sigma = 0.3$) and the second showing various mixed models with the “twin” population synthesis time delay model.

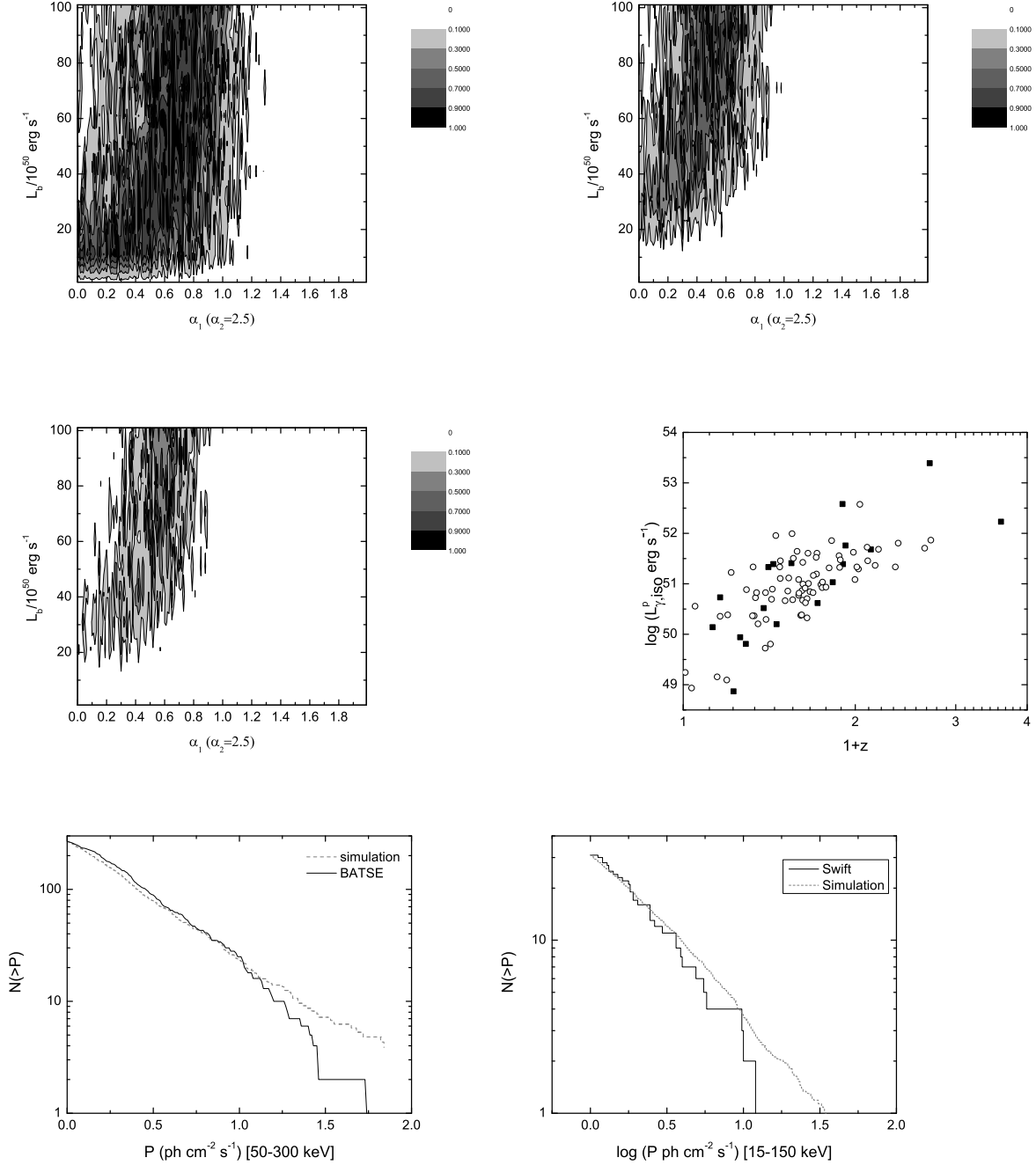


Fig. 7.— Simulation results showing a distribution of short bursts that has a merger delay timescale of 2 Gyr ($\sigma = 1.0$ Gyr), with luminosity function constrained by the $L - z$ data. The first three panels (a-c) are the $P_{KS,z}$, $P_{KS,L}$, $P_{KS,t}$ contours (darker indicates higher KS probability). Panel (d) presents the simulated GRBs (open circles) with the best fit luminosity function as compared with the data (solid dots) in the $L - z$ plane. Panel (e) and (f) shows the simulated $\log N - \log P$ (dashed line) as compared with the BATSE (solid line) and Swift data, respectively. Darker indicates higher KS probability and consistency with the observed L and z samples.

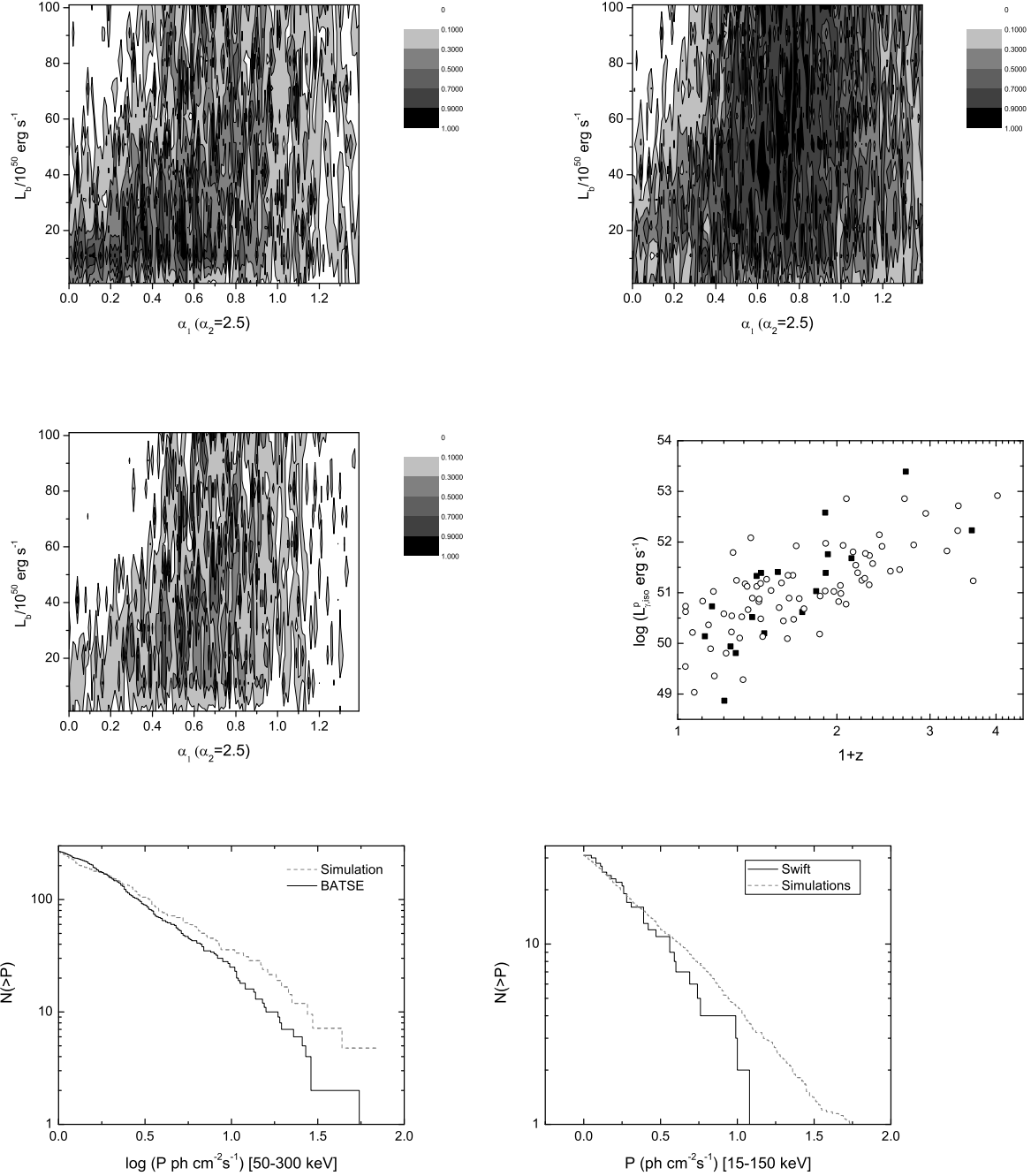


Fig. 8.— A series of contours displaying the total KS probability, $P_{KS,t}$, for a model with a mix of 30% of bursts following the star formation history and the Type II luminosity function and 70% from the ‘twin’ population synthesis model. The first three panels (a-c) are the $P_{KS,z}$, $P_{KS,L}$, $P_{KS,t}$ contours (darker indicates higher KS probability). Panel (d) presents the simulated GRBs (open circles) with the best fit luminosity function as compared with the data (solid dots) in the $L - z$ plane. Panel (e) and (f) shows the simulated $\log N - \log P$ (dashed line) as compared with the BATSE (solid line) and Swift data, respectively. Darker indicates higher KS probability and consistency with the observed L and z samples.